Communication

A Novel Theory Expression for the Impedance of a Ferrite-Loaded CW Illuminator

Peng Chen , Yangzhen Qin , Fulin Wu , Guangshuo Zhang , Qi Xu , Tianao Li , Hongmin Lu *

Posted Date: 4 August 2025

doi: 10.20944/preprints202508.0152.v1

Keywords: CW illuminators loop antenna; ferrite-loaded; antenna theory; input impedance

 doi:10.20944/preprints202508.0152.v1

Communication

A Novel Theory Expression for the Impedance of a Ferrite-Loaded CW Illuminator

Peng Chen, Yangzhen Qin, Fulin Wu, Guangshuo Zhang, Qi Xu, Tianao Li and Hongmin Lu *

School of Electronic Engineering, Xidian University, Xi'an 710071, China

* Correspondence: hmlu@mail.xidian.edu.cn

Abstract

The continuous wave (CW) illuminator, whose fundamentals are related to the theory of loop antennas loaded with ferrite materials, is an important facility for electromagnetic pulse (EMP) susceptibility assessment. However, existing theoretical formulas do not consider cases where ferrite materials are loaded into the loop antenna. This paper provides a new explicit theoretical formula of the impedance of a circular loop antenna loaded with ferrite materials for CW illuminator design and explores the variation regularity of its input impedance. Loading ferrite materials affects the internal impedance of the loop antenna and forces some modifications to the classical calculation procedure, resulting in an asymptotic numerical calculation method and a closed-form solution. The full-wave simulation results from CST Studio Suite show the maximum error is less than 0.99% compared to the classical theory. With ferrite material loaded, the input impedance of the loop antenna is significantly reduced and smoothed in a wide range ($0<k_b<2.5$). For a loop antenna with a fixed circumference, the input impedance indicates that the Q-factor decreases as the thickness of the ferrite material increases. Conversely, for a ferrite-loaded loop antenna with a constant material thickness, a larger loop circumference results in a higher Q-factor. In summary, this study provides a fast and accurate computational method for the input impedance design of CW illuminators, while also offers an effective tool for further research on the performance of ferrite-loaded loop antennas.

Keywords: CW illuminators loop antenna; ferrite-loaded; antenna theory; input impedance

1. Introduction

Loop antennas and their various modifications are widely used in applications such as UHF RFID [1–3], electromagnetic compatibility measurements [4,5], wireless power transfer [6,7], and remote sensing/geophysical exploration [8–10]. The fundamental characteristics of loop antennas were established by Storer [11] and Wu [12] in the 1950s and 1960s, respectively, who derived analytical expressions for the impedance and current distribution of unloaded thin-wire loops.

Building upon Storer and Wu's framework, McKinley [18] introduced a modified formulation that incorporates the surface impedance of metallic wires, enabling accurate impedance characterization even at optical frequencies. Subsequently, the same approach was applied to extend Izuka's theory to infrared/optical regimes for loops with periodic lumped loads [19], However, the low-frequency characteristics of the loaded loop antenna have not received sufficient attention. Recently, a specialized loop antenna, referred to as the CW illuminator, has been revisited, and a fast numerical simulation method has been proposed for calculating its field distribution [20]. Nevertheless, this work did not account for the theoretical model and the closed-form solution of the impedance.

This paper presents a novel analytical model for characterizing the input impedance of a ferrite-loaded circular loop antenna. A closed-form solution for the input impedance is derived and subsequently validated through full-wave electromagnetic simulations using three-dimensional field analysis software. The proposed model enables systematic investigation of impedance variation patterns under different loading conditions. Furthermore, this work provides an efficient and

 doi:10.20944/preprints202508.0152.v1

accurate design methodology for optimizing impedance characteristics in continuous-wave (CW) radiator applications.

2. Review of the Classical Theory of a Circular Loop

2.1. The Origin of the Problem

Figure1(a) illustrates the complete equivalent geometry of a continuous wave (CW) illuminator, which consists of a semi-elliptical structure with a delta-function source placed on the ground plane and coated with a ferrite material. In [21], the magnetic medium is initially modeled as a continuous ferrite tube enclosing the wire and subsequently simplified to discrete ferrite beads loaded along the conductor. In this work, the structure is modeled by assuming that the elliptical surface is uniformly coated with a magnetic film. From a theoretical perspective, and based on image theory, the circular loop shown in Figure 1(b) provides a reasonable approximation of the CW illuminator configuration shown in Figure1(a), provided that both loops enclose the same area.

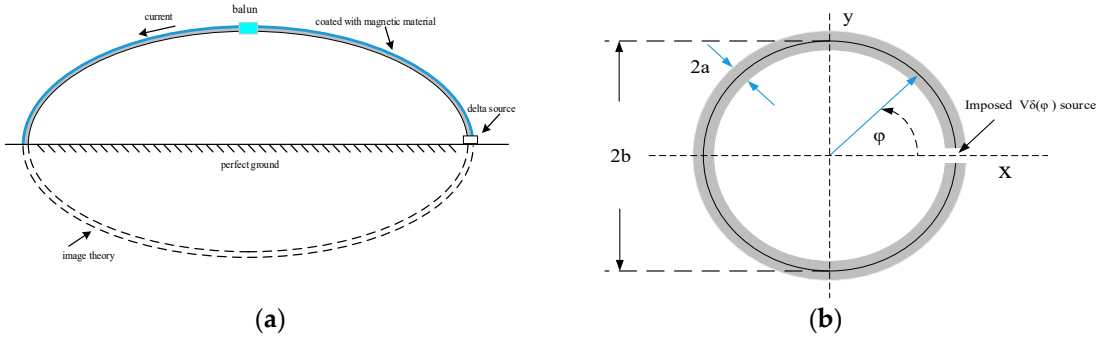

Figure 1. Geometry of (a) the CW illuminator considering the image theory and (b) the classical loop.

2.2. The Impedance of a Circular Loop Without Loads

The theoretical analysis begins with a thin circular loop, as previously studied by Storer [11] and Wu [12]. Figure1(b) illustrates the geometry and coordinate system for a metallic loop with an infinitesimal gap. The loop has a radius b and a wire radius a, and it is excited by a delta-function voltage source applied across the gap. When the condition a ≪b is satisfied, it is reasonable to assume that the surface current flows only in the azimuthal direction along the loop.

The well-known Pocklington integral equation establishes the relationship between the current distribution and the applied voltage source on an unloaded loop. It is expressed as follows [11]:

$$V\delta(\varphi)=\frac{j\zeta_0}{4\pi}\int_{-\pi}^{\pi}K(\varphi-\varphi')I(\varphi')d\varphi' \tag{1}$$

The infinite Fourier series is employed to describe the current distribution and it can be written as

$$I(\varphi)=\sum_{n=-\infty}^{\infty}I_n\exp(jn\varphi)=\frac{V\delta(\varphi)}{j\pi\xi_0}\left[\frac{1}{a_0}+2\sum_{n=1}^{\infty}\frac{\cos(n\varphi)}{a_n}\right] \tag{2}$$

where is the wave impedance in free space, a_0 … a_n are the coefficients related to the integrand in [11] and $\delta(\varphi)$ is the Dirac delta function. The loop input impedance at $\varphi=0$ is defined as

$$Z=\frac{V\delta(\varphi)}{I(\varphi)}=\frac{j\pi\xi_0}{\left[\frac{1}{a_0}+2\sum_{n=1}^{\infty}\frac{\cos(n\varphi)}{a_n}\right]} \tag{3}$$

 doi:10.20944/preprints202508.0152.v1

2.3. The Impedance of a Circular Loop Loaded with Ferrite Material

The cylindrical antenna with spatially varying internal impedance was analyzed by Wu [23]. The antenna is composed of a resistive material whose conductivity varies along its length. As current flows along the structure, the resistive material imposes a distributed opposition, effectively forming an internal impedance within the antenna.

In the present study, a circular loop antenna coated with ferrite material is considered. Based on the formulations developed by Wu and Storer [11,23,24], the current distribution on the ferrite-loaded circular loop can be expressed as follows:

$$Z_f I(\varphi) = V\delta(\varphi) - \frac{j\zeta_0}{2}\sum_{n=-\infty}^{\infty} a_n I_n \exp(jn\varphi) \tag{4}$$

where Z_f is the internal impedance caused by the loaded ferrite material in low frequency. Inserting (1) into (4) leads to

$$V\delta(\varphi) = \sum_{n=-\infty}^{\infty}\left(\frac{j\zeta_0}{2}a_n + Z_f\right) I_n \exp(jn\varphi) \tag{5}$$

Integrate on both sides of equation (5) and reduce it to

$$\begin{aligned} &\frac{1}{2\pi}\int_{-\pi}^{\pi} V\delta(\varphi)\exp(-jn\varphi)d\varphi \\ &= \frac{1}{2\pi}\int_{-\pi}^{\pi}\sum_{m=-\infty}^{\infty}\left(\frac{j\zeta_0}{2}a_m + Z_f\right) I_m \exp(jm\varphi)\exp(-jn\varphi)d\varphi \\ &I_n = \frac{V}{2\pi\left(\frac{j\zeta_0}{2}a_n + Z_f\right)} \end{aligned} \tag{6}$$

Inserting (6) into (1) and reduce it to

$$\begin{aligned} I(\varphi) &= \sum_{n=-\infty}^{\infty} I_n \exp(jn\varphi) \\ &= \sum_{n=-\infty}^{\infty}\frac{V}{2\pi\left(\frac{j\zeta_0}{2}a_n + Z_f\right)}\exp(jn\varphi) \\ &= V\left[\frac{1}{j\pi\zeta_0 a_0 + 2\pi Z_f} + \sum_{n=1}^{\infty}\frac{\cos(jn\varphi)}{\frac{j\pi\zeta_0}{2}a_n + \pi Z_f}\right] \end{aligned} \tag{7}$$

The impedance at the gap then becomes

$$\begin{aligned} Z = \frac{V}{I(\varphi=0)} &= 1/\left[\frac{1}{j\pi\zeta_0 a_0 + 2\pi Z_f} + \sum_{n=1}^{\infty}\frac{1}{\frac{j\pi\zeta_0}{2}a_n + \pi Z_f}\right] \\ &= 1/\left[\frac{1}{Z_0'} + \sum_{n=1}^{\infty}\frac{1}{Z_n'}\right] \end{aligned} \tag{8}$$

where

$$Z_0' = j\pi\zeta_0 a_0 + 2\pi Z_f \tag{9}$$

$$Z_n' = j\pi\zeta_0(a_n/2) + \pi Z_f \tag{10}$$

 doi:10.20944/preprints202508.0152.v1

3. Analysis of the Internal Impedance

3.1. The Dispersion Characteristic of Ferrites

The impedance of the ferrite-loaded loop is expressed in (8), where the internal impedance term Z_f requires further derivation. At low frequencies—where ferrite materials exhibit significant magnetic activity—the interaction between ferrite and the loop wire is illustrated in Figure 2. In this frequency range, the current flowing through the loop is reduced due to two primary mechanisms: energy is consumed in establishing the magnetic flux within the ferrite material, and additional energy is dissipated as losses within the ferrite itself.

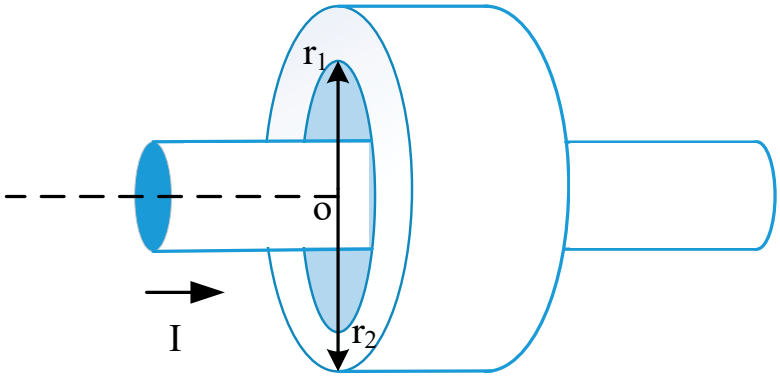

Figure 2. The interaction between ferrite and the loop wire.

The impedance of ferrite beads presented to a loop is expressed as [25]

$$Z_f = j\omega\left[\frac{\mu_0}{2\pi}\ln\left(\frac{r_2}{r_1}\right)\right]\mu_r \bullet 2\pi b \quad (11)$$

where r_1,r_2 are the inner radius and outer radius of a ferrite bead loading on a loop respectively,μ_r is the relative permeability.

Since the impedance of a ferrite bead is directly influenced by its magnetic permeability characteristics, it is essential to investigate the underlying magnetization mechanisms and the frequency-dependent dispersion behavior of permeability. Extensive research has been conducted on magnetic materials, particularly Ni-Zn and Mn-Zn ferrites [26,27].

As reported by Takanori in [26], two distinct types of magnetic resonance appear in the permeability spectra of Ni-Zn and Mn-Zn ferrites. These resonances are attributed to domain wall motion and spin rotation, respectively. By superimposing the contributions from both mechanisms, the complex relative permeability of these ferrites can be modeled as:

$$\mu_r = 1 + \chi_d + \chi_s = 1 + \frac{\omega_d^2 \chi_{d0}}{\omega_d^2 + \omega + i\omega\beta} + \frac{(\omega_s + i\omega\alpha)\omega_s \chi_{s0}}{(\omega_s + i\omega\alpha)^2 - \omega^2} \quad (12)$$

The parameters are listed as follows

- χ_d domain-wall motion magnetic susceptibility
- χ_s spin motion magnetic susceptibility
- χ_{d0} static magnetic susceptibility for domain-wall component
- χ_{s0} static magnetic susceptibility for spin component
- ω_d resonance frequency of domain-wall component
- ω_s resonance frequency of spin component;

Inserting equation (12) into (11) leads to

 doi:10.20944/preprints202508.0152.v1

$$Z_f = j\omega\left[\frac{\mu_0}{2\pi}\ln\left(\frac{r_2}{r_1}\right)\right]\left(1+\frac{\omega_d^2\chi_{d0}}{\omega_d^2+\omega+i\omega\beta}+\frac{(\omega_s+i\omega\alpha)\omega_s\chi_{s0}}{(\omega_s+i\omega\alpha)^2-\omega^2}\right)\bullet 2\pi b \quad (13)$$

The ferrite model parameters in [25] is illustrated in Table 1 and the Mn-Zn parameters are adopted for theory analysis.

Table 1. ferrite model parameters.

Ferrite material	Density(g/cc)	Domain wall component			Spin component		
		χ_{d0}	ω_d (MHz)	β	χ_{s0}	ω_s (MHz)	α
Mn-Zn Ferrite	4.90	3282	2.5	9.3×10^6	1438	6.3	1.28
Ni-Zn Ferrite	5.20	485	2.8	3.5×10^6	1130	1100	161

3.2. Comparison of the Surface and Ferrite Impedance

The surface impedance of a cylindrical conductor becomes negligible at low frequencies but becomes significant in the optical frequency range. In contrast, the impedance contribution from ferrite materials is dominant at low frequencies and diminishes as the frequency increases. These distinct impedance behaviors are primarily governed by the permittivity of the conductor [18] and the permeability of the ferrite, respectively.

According to the literature [27,28], both elastic oscillations and interband transitions of the electron gas in metals contribute to the frequency-dependent permittivity. These mechanisms are effectively captured by analytical models. Similarly, in ferrite materials, the motion of magnetic domains exhibits behavior analogous to the electron gas in metals. Domain wall motion corresponds to elastic oscillation, while spin dynamics and resonance bandwidth transitions share a similar mathematical representation [26].

As a result, the impedance characteristics of a ferrite-loaded circular loop become particularly prominent at low frequencies. The introduction of ferrite material leads to a smoother overall impedance profile and reduces the input impedance of the antenna, thereby facilitating improved impedance matching. Figure 3 shows the magnitude of ferrite-loaded loop impedance. For a ferrite-loaded loop antenna with a fixed thickness ratio of b/a=64, the magnitude of the input impedance gradually decreases and becomes smoother as the ferrite material thickness d is reduced.

 doi:10.20944/preprints202508.0152.v1

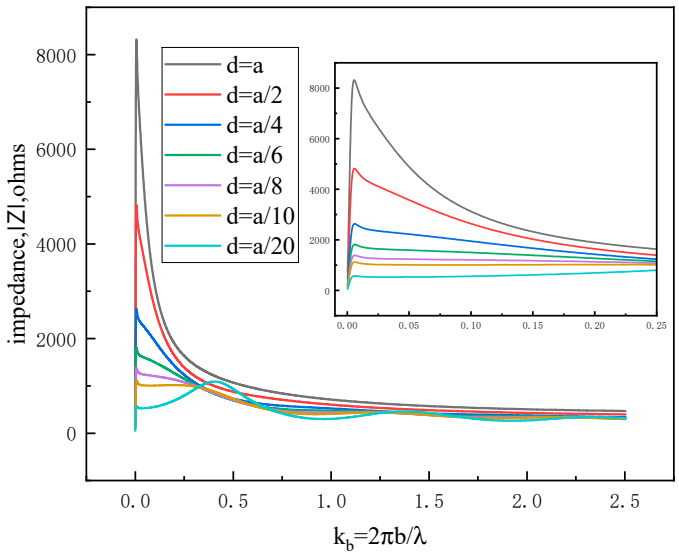

Figure 3. The magnitude of impedance varying with d.

4. Validations of the Proposed Impedance Formulation

4.1. The evaluation of the Loop Impedance with Ferrite Loads

For loops without ferrite loading, the impedance is given by (2). Storer [11] provided an approximate expression for the parameter a_n when the mode number n>5, as follows:

$$a_n \approx \frac{1}{\pi}\left(k_b - \frac{n^2}{k_b}\right)\left(\ln\left(\frac{2b}{a}e^{-0.5772}\right) - \ln(n) - j\times\frac{(k_b)^{2n+1}}{\Gamma(2n+2)}\right) n > k_b, n \gg 1 \tag{14}$$

He subsequently replaced the summation over terms for n>5 with an integral representation. Following a series of analytical derivations, the integral was evaluated as:

$$\Psi = 2\sum_{n=5}^{\infty}\frac{\cos(n\varphi)}{a_n} = \frac{2\pi}{\ln\left(\frac{n_0}{4.5}\right)}\frac{k_b}{4.5}\left[J + \frac{1}{3}\left(\frac{k_b}{4.5}\right)^2\right] \tag{15}$$

where $J = (0.47, 0.9, 1.25, 1.4, 1.4)$ for $\Omega = (8, 9, 10, 11, 12)$, $n_0 = 2b/a\exp(-0.5772)$.

The impedance expression in (8) is analytically complex and not easily evaluated through closed-form derivation. To approximate the impedance, a numerical computation approach is employed. Given that the current on the loop is continuous and bounded, the resulting series is convergent. Furthermore, as n increases, the summation over terms with *n*>5 approaches a constant function that depends solely on the product k_b. Accordingly, the impedance can be reformulated as:

$$Z = \frac{V}{I(\varphi = 0)} = 1/\left[\frac{1}{Z_0^{'}} + \sum_{n=1}^{4}\frac{1}{Z_n^{'}} + \psi(k_b)\right] \tag{16}$$

Given that the first five terms in (15) are explicitly known, the remaining task is to estimate the residual sum. According to the Euler–Maclaurin formula, the summation can be approximated by an integral, which yields the following expression:

$$\psi(k_b) = \sum_{n=5}^{N} f(n) = \sum_{n=5}^{N}\frac{1}{Z_n^{'}} \approx \int_5^N f(x)dx + \frac{(f(5) + f(N))}{2}, \quad N \to \infty \tag{17}$$

 doi:10.20944/preprints202508.0152.v1

Substitute (10), (13) into (16) and reduce it

$$\begin{aligned}\psi(k_b) &\approx \int_5^N \frac{1}{j\pi\zeta_0\left(\frac{1}{\pi}\left(k_b-\frac{n^2}{k_b}\right)\left(\ln\left(\frac{2b}{an}e^{-0.5772}\right)-j\times\frac{(k_b)^{2n+1}}{\Gamma(2n+2)}\right)\Big/2\right)+\pi Z_f}dx \\ &+\frac{f(N)+f(5)}{2} \\ &\approx \psi_0+\frac{f(5)}{2}\end{aligned} \tag{18}$$

where a, b are the wire radius and loop radius respectively, and $k_b = 2\pi b/\lambda$.

A numerical program was implemented to compute the first term in (17), ψ_0, for N=100,150,200,250 and 300. Figure 4(a) illustrates the asymptotic behavior of the real and imaginary components of ψ_0 as N increases. A comparison between the numerical results and the analytical expression given in (14) is presented in Figure 4(b), where the relative error is observed to be less than 0.99%.

As shown in Figure 4(a), both the real and imaginary components of ψ_0 exhibit approximately linear behavior. The imaginary component intersects the points (0, 0) and (2.5, 1.7e-3), while the real component passes through (0, 0) and (2.5, 5.8e-4). Based on these observations, the approximate linear expression for ψ_0 can be derived as:

This section may be divided by subheadings. It should provide a concise and precise description of the experimental results, their interpretation, as well as the experimental conclusions that can be drawn.

$$\psi(k_b) \approx \frac{(0.58+j1.7)}{2.5}\times 10^{-3}k_b + \frac{\left(f(\infty)+f(5)\right)}{2} \tag{19}$$

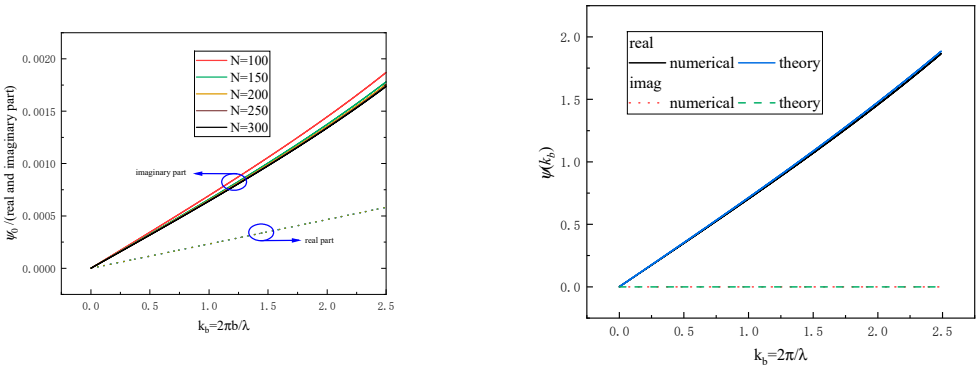

(**a**) (**b**)

Figure 4. Numerical calculations of ψ_0 for (a) loop loaded with ferrite and (b) loop without loads.

4.2. Comparison Between Theoretical and Simulated Impedance of the Ferrite-Loaded Loop

To validate the closed-form impedance expressions proposed in this study, numerical results are compared with full-wave simulations performed using CST Microwave Studio. The input impedance of the ferrite-loaded loop antenna obtained from the analytical solution is compared with the results from CST simulation in Figure 5, showing excellent agreement between the two. The loop antenna has a radius of 304.8 mm and a wire diameter of 4.8 mm, while the ferrite material features a thickness of 0.625 mm. Due to the limited accuracy of the time-domain solver in CST for low-frequency problems, the frequency-domain solver was employed during the validation process.

 doi:10.20944/preprints202508.0152.v1

This section may be divided by subheadings. It should provide a concise and precise description of the experimental results, their interpretation, as well as the experimental conclusions that can be drawn.

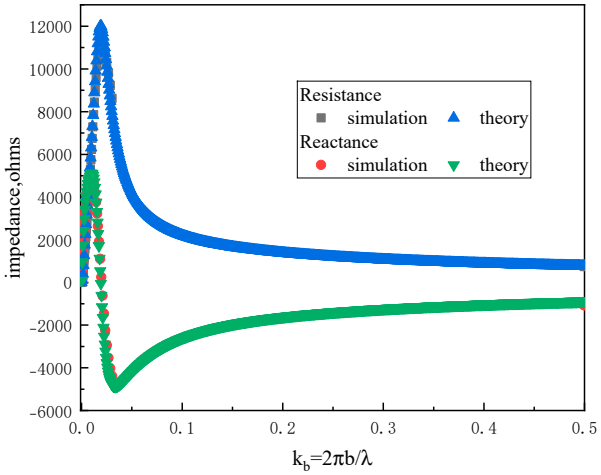

Figure 5. Comparison of results from simulation and theory, with $\Omega = 2\,ln\left(\frac{2\pi b}{a}\right) = 12$.

5. Conclusions

For an unloaded thin loop antenna, its characteristics can be accurately described using classical theory. However, for specific applications, it becomes necessary to load the antenna with ferrite material and derive a theoretical expression for its input impedance. In this work, a new impedance expression is proposed by introducing an additional term to the unloaded case. Comparisons with CST simulation results are conducted to validate the theoretical model. Overall, the proposed expression shows good agreement with simulation in the range $0<kb<2.5$. The results presented in this paper can be utilized for the rapid computation of the input impedance of ferrite-loaded loop antennas and for the design of impedance matching networks.

The ferrite loading influences the antenna impedance by affecting the current distribution. The underlying physical mechanisms include spin rotation and magnetic domain wall motion, which contribute to the dispersive behavior of the ferrite material. The permeability data used in the CST simulations is based on a model proposed in [25].

Author Contributions: Conceptualization, H.L., and P.C.; methodology, P.C.; software, P.C. and F.W.; validation, Y.Q.; data curation, P.C. and Y.Q.; writing—original draft preparation, P.C.; writing—review and editing, H.L. All authors have read and agreed to the published version of the manuscript.

Funding: This research was funded by the National Defense Basic Research Project, grant number MKF20230377

Data Availability Statement: The datasets generated and analyzed during the current study are not publicly available but are available from the corresponding author on reasonable request.

Acknowledgments: The authors would like to express their sincere gratitude to Jinghai Guo, Dongyang Sun from northwest institute of nuclear technology (NINT) for their valuable support in both the experimental work and theoretical derivations of this study. Their insightful guidance and constructive suggestions have significantly contributed to the quality and depth of this research.

Conflicts of Interest: The authors declare no conflicts of interest. The funders had no role in the design of the study.

 doi:10.20944/preprints202508.0152.v1

References

1. Chenyang, S.;. Zhipeng, W. "A Loop Antenna Array with an Enlarged Near-Field Interrogation Zone for UHF RFID Near-Field and Far-Field Applications," *IEEE Trans. Antennas and Wireless Propagation Letters*, vol. 21, no. 10, pp. 1985–1989.
2. Pavel, T.M.; Irina, D.; Michail, V.O.; Irina V. "Electrically Small Loop Antennas for RFID Applications," *IEEE Trans. Antennas and Wireless Propagation Letters*, vol. 14, pp. 1786–1789.
3. Bijaya, S.E.A; Leena, U. "UHF RFID Reader Antenna for Near-Field and Far-Field Operations," *IEEE Trans. Antennas and Wireless Propagation Letters*, vol. 10, pp. 1274–1277.
4. Carlo, F. M.C.; Alessio, B. "Electromotive Force Induced in and Inductance of an Electrically Small Circular Loop Antenna," *IEEE Transactions on Electromagnetic Compatibility*, vol. 56, no. 4, pp. 780–783.
5. IEEE Standard Method for Measuring the Effectiveness of Electromagnetic Shielding Enclosures, IEEE Std 299™, 2006.
6. Mohamed, M.; Konstanty, B.; Beadaa, M.; Amin, A. "Wireless Power Link Based on Inductive Coupling for Brain Implantable Medical Devices," *IEEE Antennas and Wireless Propagation Letters*, vol. 17, no. 1, pp. 160–163.
7. Lee, W.S.; Oh, K.S.; Yu, J.W. "Field Analysis and Measurement of Antiparallel Resonant Loop for Wireless Charging," *IEEE Antennas and Wireless Propagation Letters*, vol. 14, pp. 1459–1462.
8. Parise, M. "An Exact Series Representation for the EM Field from a Circular Loop Antenna on a Lossy Half-Space," *IEEE Antennas and Wireless Propagation Letters*, vol. 13, pp. 23–23.
9. Ronold, W. P. K.; Owens, M.; Wu, T.T. "Historical and Technical Overview of Electromagnetic Surface Waves; Introduction to Lateral Waves," in Lateral Electromagnetic Waves, 1st ed., New York, NY, USA: Springer-Verlag, 1992, pp. 1–23.
10. Mauro, P.; Daniele, R.; Giulio, A. "Loop Impedance of Single-Turn Circular Coils Lying on Conducting Media," *IEEE Transactions on Electromagnetic Compatibility*, vol. 64, No. 2, pp. 580–584.
11. James, E.S. "Impedance of thin-wire loop antennas," *Transactions of the American Institute of Electrical Engineers*, vol. 75, No. 5, pp. 606–619.
12. Wu, W. T. "Theory of the Thin Circular Loop Antenna," *Journal of Mathematical Physics*, vol. 3, no. 6, pp. 1301–1304,.
13. Iizuka, K. "The circular loop antenna multiloaded with positive and negative resistors," *IEEE Transactions on Antennas and Propagation*, vol. 13, no. 1, pp. 7–20,.
14. .Pendry, J. B; Holden, A. J ; Robbins, D. J, "Magnetism from conductors and enhanced nonlinear phenomena," *IEEE Transactions on Microwave Theory and Techniques*, vol. 47, no. 11, pp. 2075–2084.
15. Hanson, G. W, "On the applicability of the surface impedance integral equation for optical and near infrared copper dipole antennas," *IEEE Transactions on Antennas and Propagation*, vol. 54, no. 12, pp. 3677–3685.
16. DeAngelis C. "Extending antenna theory to the optical domain," in Proceedings of the 2009 European Microwave Conference, Rome, Italy, Sept. 29–Oct. 1, 2009, pp. 810–813.
17. . McKinley, A. F.; White, T. P.;.Maksymov, I. S.; Catchpole, K. R. "The analytical basis for the resonances and anti-resonances of loop antennas and meta-material ring resonators," *Journal of Applied Physics*, vol. 112, no. 9.
18. McKinley, A. F.; White, T. P;. Catchpole, K. R, "Theory of the circular closed loop antenna in the terahertz, infrared, and optical regions," Journal of Applied Physics, vol. 114, no. 4.
19. Arnold, F. M, "Theory of impedance loaded loop antennas and nanorings from RF to optical wavelengths," *IEEE Transactions on Antennas and Propagation*, vol. 65, no. 5, pp. 2276–2281.
20. Qi, Z.; . Zhongyuan, Z.; Yixing, G.; Mingjie, S.; Peng H. ; and Yang X. "An Algorithm for Fast Simulation of CW Illuminator," *IEEE Transactions on Electromagnetic Compatibility*, vol. 64, no. 6, pp. 2104–2111.
21. Baum, C. E; Prather, W. D. "Topology for transmitting low-level signals from ground level to antenna excitation position in hybrid EMP simulators," Sensor and Simulation Notes, Note 333, Air Force Weapons Laboratory, Kirtland AFB, NM, Sep. 30, 1991.

 doi:10.20944/preprints202508.0152.v1

22. .Prather, W. D.; Rooney, M. R.; Cafferky, J.;. Rynne, T. M.; Ortiz, L. ; Anderson, G. "Swept CW testing of shielded systems," in 2012 IEEE International Symposium on Electromagnetic Compatibility, Montreal, QC, Canada, Aug. 6–10, 2012, pp. 657–662.
23. Wu, T; King, R. "The cylindrical antenna with nonreflecting resistive loading," *IEEE Transactions on Antennas and Propagation*, vol. 13, no. 3, pp. 369–373, May 1965..
24. Prather, W. D. "Ellipticus ferrite/resistive loading," Measurement Notes, Note 41, 1993.
25. Takanori, T.; Masahiro, U.; Toshihiko, T.; Tatsuya N.; Kenichi, H. "Frequency dispersion and temperature variation of complex permeability of Ni-Zn ferrite composite materials," Journal of Applied Physics, vol. 78, no. 6, pp. 3997–3999, Sept. 1995.
26. Takanori, T.; Tatsuya, N.; Kenichi, H. "Magnetic field effect on the complex permeability spectra in a Ni–Zn ferrite," *Journal of Applied Physics*, vol. 82, no. 6, pp. 2947–2951.
27. Novotny, L.; Hecht, B. "surface plasmons," in Principles of Nano-Optics, 2nd ed. Cambridge, UK: Cambridge University Press, 2012. pp. 374–376.
28. Etchegoin, P. G.; Le Ru, E. C; Meyer, M."An analytic model for the optical properties of gold," *Journal of Chemical Physics*, vol. 125, no. 16, pp. 164705, Oct. 2006.
29. Author 1, A.B. Title of Thesis. Level of Thesis, Degree-Granting University, Location of University, Date of Completion.
30. Title of Site. Available online: URL (accessed on Day Month Year).